JOURNAL OF ELECTRON MICROSCOPY TECHNIQUE 8:297-306 (1988)

High-Resolution Electron Microscopy of High-Temperature Superconductors

L.D. MARKS, D.J. LI, H. SHIBAHARA, AND J.P. ZHANG
Materials Research Center, Northwestern University, Evanston, Illinois 60208

KEY WORDS Defects, Polymorphs, Structure

ABSTRACT We review recent results obtained at Northwestern using high-resolution electron microscopy to study high-temperature superconductors. While in general these materials form large, very perfect single crystal grains which display very few imperfections, there is also evidence of slip defects, amorphous regions, and order-disorder transformations. We also report that the gadolinium-based superconductors and in one case yttrium-based superconductors show evidence for some copper solid solubility in the form of copper-rich planar defects. The structure of a metastable trigonal polytype is also reported, as are the effects of electron beam and water vapor damage to the materials.

INTRODUCTION

The recent wave of high-temperature ceramic superconductors, most notably the triple perovskite $YBa_2Cu_3O_{7-\delta}$ (generally abbreviated to 123) and its derivatives where the yttrium is replaced by almost any rare earth ion, have raised a number of important questions for electron microscopists. Perhaps of primary importance is why some preparations yield "good" superconductors, while others do not, and why bulk preparation techniques have to date yielded specimens that fail to match the current-carrying capacity of thin film specimens. Is this due to internal defects, secondary phases, or perhaps grain boundary phases in some of the materials? In addition, do these defects or secondary phases, if present, change as a function of processing of the ceramics?

For the last few months we have been fairly intensively studying these conventionally produced powder superconductors at Northwestern (Hwu et al., 1987a,b), using as our primary tool high-resolution electron microscopy supplemented with some microanalysis and diffraction. To a certain extent many of our results are somewhat negative; we have been unable to find any clear-cut structural features that could be responsible for poor behavior. What we have found are some interesting structural variations and defects which might in some cases lead to degradation of the properties. In this paper we will briefly review our results to date on the perfect superconductor, planar slip defects, copper-rich defects, order-disorder phenomena, polymorphs, and the effects of electron beam and water vapor damage. A short report on some of these results has already appeared (Buckett et al., 1987; Marks et al., 1987), and more detailed reports of other parts of the work are in preparation (Li and Zhang; Zhang et al.; Shibahara et al.)

EXPERIMENTAL METHOD

Superconductor specimens were prepared by the standared repeated annealing, grinding procedure and then cooled slowly in air (see, for instance, Hwu et al., 1987a,b). We have explored only the $YBa_2Cu_3O_7$ compound and the related $GdBa_2Cu_3O_7$ material which has been shown by a number of authors (e.g., Fisk et al., 1987; Hor et al., 1987; Hulliger and Ott, 1987) to be an equivalent superconductor. As a rule Meissner and conductivity measurements were used to check the properties of the specimens. To explore metastable and defective phases, superconducting specimens were prepared by quenching both in liquid nitrogen and oil. The specimens were then *very* gently ground (typ-

Received October 26, 1987; accepted November 9, 1987.

Address reprint requests to L.D. Marks, Materials Research Center, Northwestern University, Evanston, IL 60208.

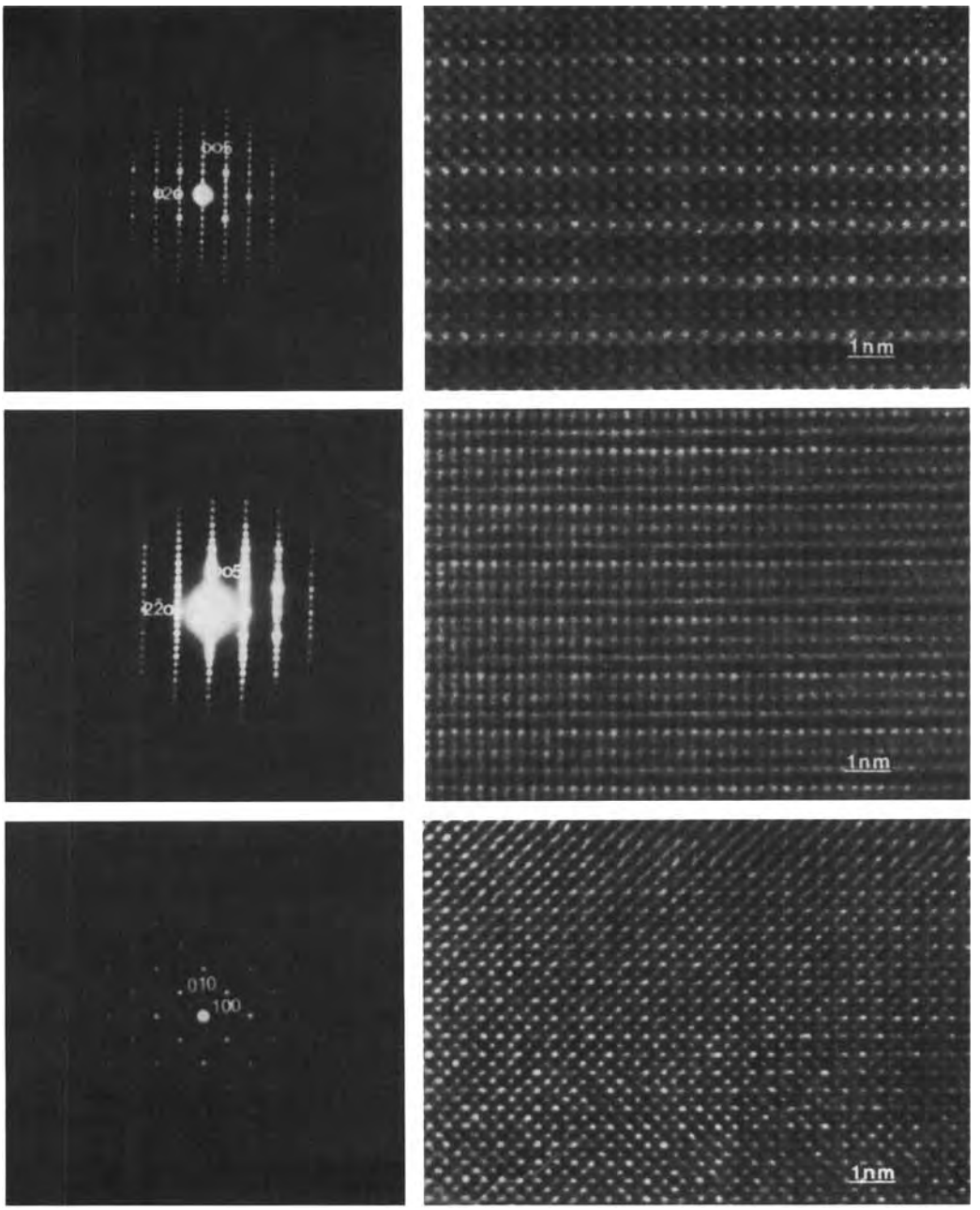

Fig. 1. Images of the triple perovskite structure taken along the three major zones, from top to bottom [100], [110], and [001], with diffraction patterns on the left.

ically between two glass plates) in order to minimize mechanical deformation, mounted on pyrolized carbon films, baked briefly on a light bulb for 10 minutes to reduce surface hydrocarbons, and then examined in either a Hitachi 700 at 200 kV or a Hitachi H-9000 operated at 300 kV. To check on the image interpretation, images were stimulated on

an Apollo workstation ring using programs written by one of us (L.D.M.) which are interface to SEMPER routines operating on the 1,024 × 1,024-pixel displays of Apollo 660 workstations. Conditions for the calculation were a slice thickness of 0.28 to 0.2 nm sampled to about 6 nm^{-1} in reciprocal space with a Cs of 0.9 mm at 300 kV, a focal spread of 8 nm, and a convergence of 0.5 to 1.0 mr.

Perfect superconductor

The main component of the specimens prepared by slow cooling in oxygen is the perfect triple perovskite—see, for instance, Figure 1 and Marks et al. (1987). Typically traces of one or two impurity phases are present in a well-prepared specimen owing to slight deviations from the true 123 metal compostion and/or incomplete mixing; less careful preparation in our experience introduced more impurity phases. Image simulations indicate that the material has the structure originally determined by X-ray (Hazen et al., 1987; Siegrist et al., 1987) and neutron diffraction (Beech et al., 1987; Beno et al., 1987; Greedan et al., 1987); the basic structure of the 123 compound is a solved question, so it is overkill to go to the length of very detailed image simulations to detect all the atomic positions. As observed by numerous authors (see, for instance, other papers in this volume and the papers by Beyers et al., 1987; Hewat et al., 1987; Hyde et al., 1987) the orthorhombic phase is normally twinned on (110) planes, presumably a stress-relief process during the tetragonal to orthorhombic phase transition; this can clearly be seen by splitting of the higher-angle diffraction spots. One exception to the general result of the perfect perovskite structure should be noted here; in thin film specimens (courtesy of workers at Stanford University) preliminary results indicate that there are extensive amorphous regions.

Tetragonal phase

As a rule, most of the specimen has the perfect structure shown above, and further analysis is unwarranted, as mentioned above, since X-ray and neutron diffraction methods are superior to imaging methods for perfect

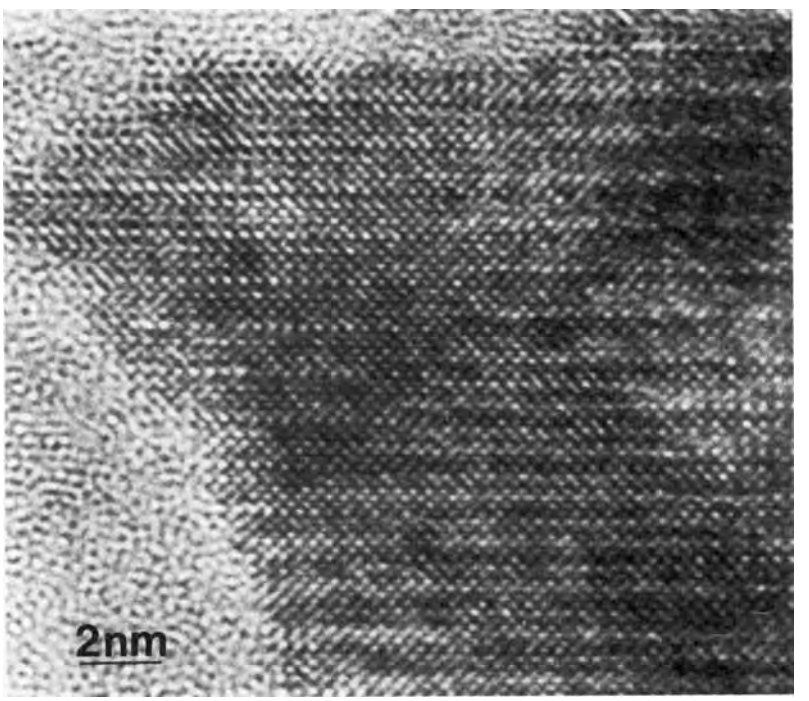

Fig. 2. Image taken along the [100] zone of the tetragonal phase.

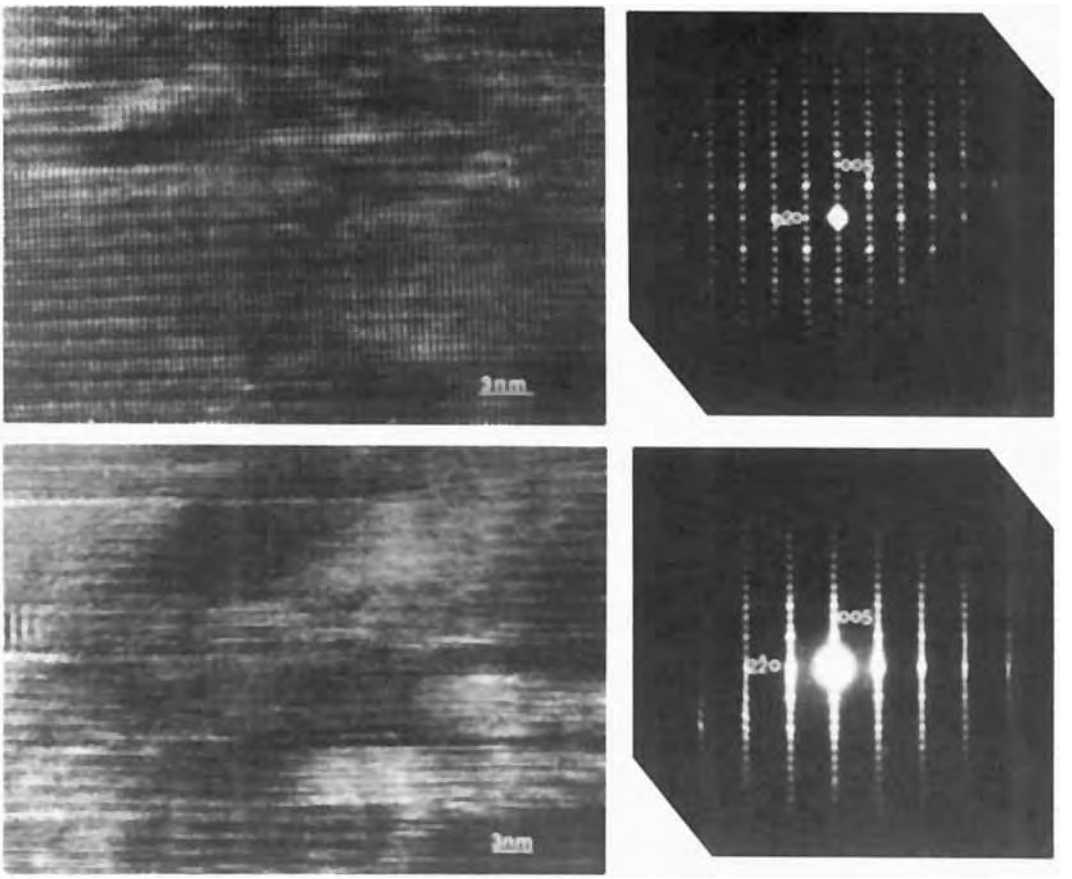

Fig. 3. Images showing planar slip defects lying on (001) planes caused by mechanical deformation: **top)** [100] zone and **bottom)** [110] zone.

structures. The thrust of our research, therefore, turned towards defects, either native to the structure or produced by varying the preparation conditions. The first experiment that was tried was liquid nitrogen quenching, which is known to produce a non-superconducting tetragonal structure with an average oxygen content of <6.5 atoms. The resultant structure (Fig. 2) is essentially the same as that of the orthorhombic phase, as also observed by X-ray methods (e.g., Gallagher et al., 1987).

Slip defects

In general, the material as mentioned above is rather perfect. One exception to this is that planar defects and in some cases cracks can often be found along (001) planes near to the surface of very thin flakes as shown in Figure 3. These defects can be understood as due to slip normal to the c-axis, caused by mechanical deformation during grinding to prepare the high-resolution specimens; only the thin flakes, not the thicker regions, show these defects. An earlier observation of similar defects by Ourmazd et al. (1987), who suggested that they could be the source of the superconductivity, can be attributed to use of room-temperature ion-beam milling to produce samples; we (Marks et al., 1987) along with a number of other authors (Hewat et al., 1987; Hyde et al., 1987) are confident that these defects are just an artifact. As further confirmation that the (001) plane is a preferred slip plane it should be noted that sinter-forged specimens are highly textured with the c-axis parallel to the pressing direction (Robinson et al., 1987).

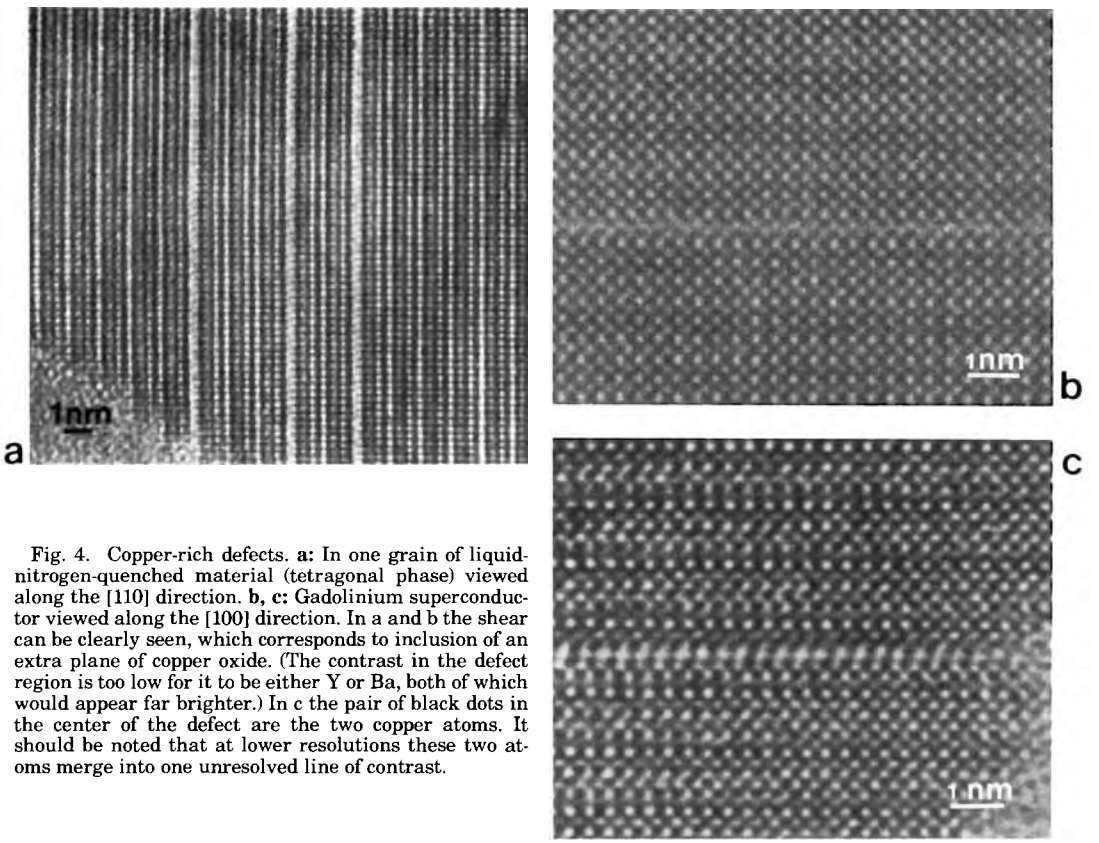

Fig. 4. Copper-rich defects. **a:** In one grain of liquid-nitrogen-quenched material (tetragonal phase) viewed along the [110] direction. **b, c:** Gadolinium superconductor viewed along the [100] direction. In a and b the shear can be clearly seen, which corresponds to inclusion of an extra plane of copper oxide. (The contrast in the defect region is too low for it to be either Y or Ba, both of which would appear far brighter.) In c the pair of black dots in the center of the defect are the two copper atoms. It should be noted that at lower resolutions these two atoms merge into one unresolved line of contrast.

Copper rich defects

While the slip defects were the only defects that are common in the yttrium superconductor, two other defect structures can occur, both of which indicate that it is possible to obtain some copper solid solubility in the system. In one, *and only one* grain of liquid-nitrogen-quenched yttrium superconductor the defects shown in Figure 3a were observed. Quite commonly in the gadolinium superconductor we observed (Shibahara et al., in preparation) the defects shown in Figure 4b, 4c. The defects in Figure 4a,b correspond to an additional copper plane and a shear of approximately 1/6[331], essentially an antiphase domain boundary. The other defect shown in Figure 4c corresponds to a displacement along the c-axis with two Cu atoms in a line. At present there is no data on the GdBaCu oxide phase diagram so we cannot clearly understand the significance of the latter results, except to note the difference relative to the yttrium superconductor where it is established that the 123 compound is a stable point phase (e.g., Wang et al., 1987). It should be mentioned that Zandbergen et al. (1987) have reported similar defects in $ErBa_2Cu_3O_7$ taken using a JEOL 200CX, describing them as additional planes of Er, which does not agree with our conclusions.

Order-disorder and polytypism

One of our first observations of these materials was that there existed classical order-disorder transformations [1]. The perfect structure has the Ba and Y atoms ordered on the (100) planes of the perovskite parent cell, but some regions (see Fig. 5) showed loss of the triple periodicity, implying random distribution of the Y and Ba atoms. (Initially this region showed some partially ordered regions when viewed using a TV pickup system, but these degenerated rapidly in the

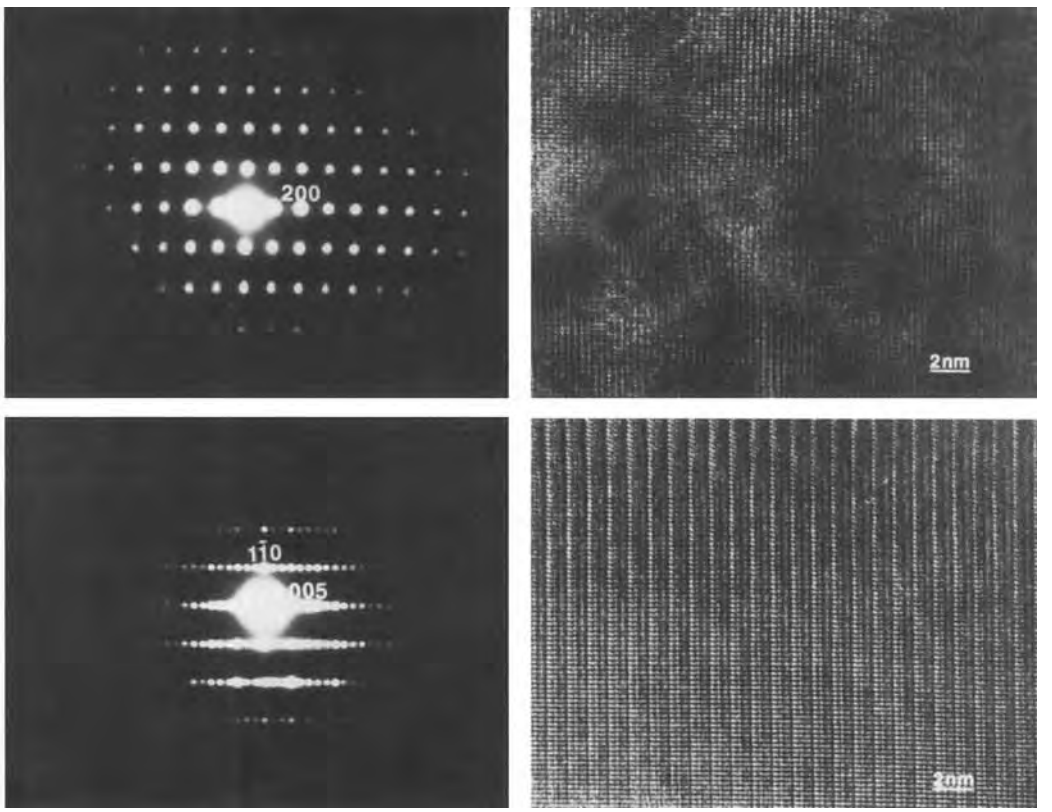

Fig. 5. **Top:** Image and diffraction pattern of a region showing loss of the triple perovskite superstructure. Growing from this region was a grain of perfect 123, which is shown at the bottom with its diffraction pattern.

electron beam.) This occurred in some grains from which the perfectly ordered phase appeared to be growing, although there were some indications from EDX analysis that these regions might be yttrium deficient.

A more recent result (Li and Zhang, in preparation) confirms the idea that the Y and Ba atoms need not be ordered in the structure of $YBa_2Cu_3O_{6.5}$ produced by quenching in oil (oil is a much faster quencher than liquid nitrogen). The resultant material (see Fig. 6) is a combination of very small regions of two trigonal phases with lattice parameters of a=0.536 and c=0.666 nm, the first having P3m1 symmetry with the Y atoms stacked along (111) planes of the parent perovskite, while the second has P3m1 symmetry and the same arrangement of atoms except that there is interchange of the Y atoms and one of the Cu sites within the unit cell as shown in Table 1. We believe that at high temperature the entropically favored structure will be a fully disordered structure with the yttrium and barium completely disordered in a simple perovskite structure. During quenching, as an alternative to the true 123 ordering along [001], some ordering can occur on (111) planes leading to these metastable trigonal phases. On slower cooling, the lower energy ordering along [001] takes place.

Electron beam and water damage

Although many of the better yttrium superconducting specimens are quite beam resistant, some, primarily those with a lower oxygen content, damage in the beam (Zhang et al., in preparation). The initial consequence is the formation of an amorphous surface phase (see Fig. 7a), which grows in from the surface. This is followed by segregation of the barium to the surface in the form of barium oxide (see Fig. 7b). The polytypic phase shown in Figure 6 also damages, with no amorphous phase formation but instead a loss of chemical ordering and segregation to

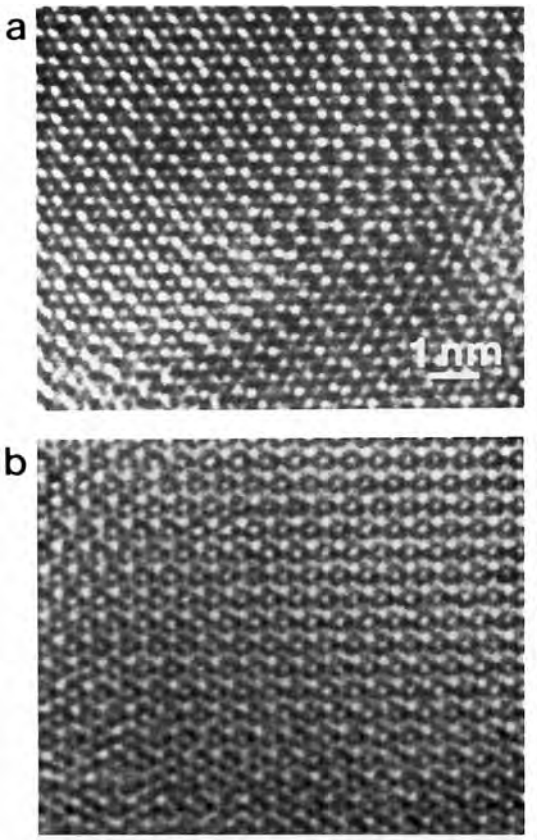

Fig. 6. Trigonal phases found in oil-quenched superconductor: a) P3m1 and b) P$\bar{3}$m1, both viewed along the [001] zone.

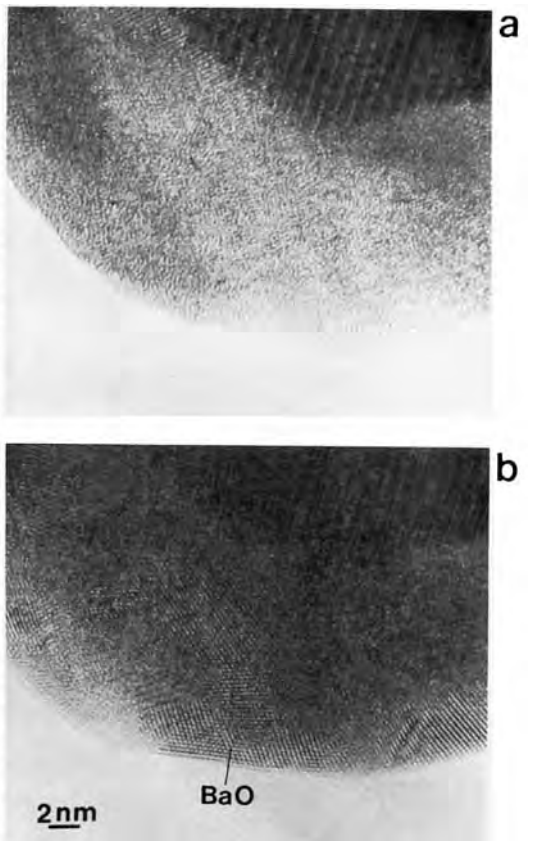

Fig. 7. Effects of electron beam: a) amorphous phase produced at the surface and b) BaO formed on further irradiation.

TABLE 1. Positions of the metal atoms in the two trigonal polymorphs of $YBa_2Cu_3O_{6.5}$[1]

Atoms	Sites	x	y	z	Occupancy
P$\bar{3}$m1					
Y	1(a)	0	0	0	1
Ba	2(d)	1/3	2/3	1/3	1
Cu	1(b)	0	0	1/2	1
Cu	2(d)	1/3	2/3	5/6	1
O	3(e)	0	1/2	0	0.7
O	6(i)	1/3	1/6	1/3	0.7
P3m1					
Y	1(b)	1/3	2/3	5/6	1
Ba	1(b)	1/3	2/3	1/3	1
Ba	1(c)	2/3	1/3	2/3	1
Cu	1(a)	0	0	0	1
Cu	1(a)	0	0	1/2	1
Cu	1(c)	2/3	1/3	1/6	1
O	3(e)	0	1/2	0	0.7
O	6(i)	1/3	1/6	1/3	0.7

[1]These data are based upon matching the diffraction patterns from single grains taken over a large range of angles and matching to the experimental images. The oxygen content was determined by RGA, and the oxygen positions have been taken from the basic perovskite lattice.

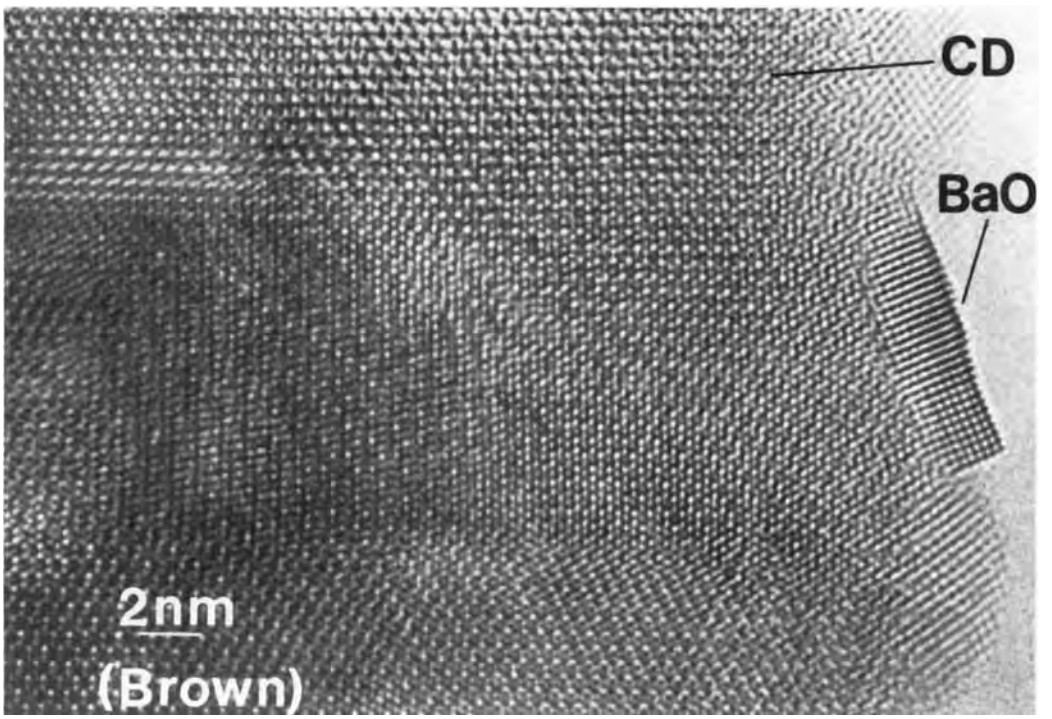

Fig. 8. Image of the trigonal phase showing the formation of BaO at the surface.

produce barium oxide on the surface (see Fig. 8). Two processes appear to be important, namely, diffusion of the barium atoms and oxygen DIET (desorption induced by electronic transitions; see, for instance, Petford et al., 1986). We suspect that some oxygen loss destabilizes the triple perovskite structure, which makes more space available for barium diffusion. Two other reports in the literature confirm this idea; Eaglesham et al. (1987) report an orthorhombic to tetragonal phase transition in the beam, which indicates oxygen loss, while Hyde et al. (1987) report the formation planar defects which would be expected from barium diffusion. Presumably, in the less oxygen-deficient samples the oxygen diffusion rate is slower, which reduces sharply the rate of damage. (Oxygen ejection solely from the immediate surface will have little effect unless the oxygen can be replenished by diffusion.)

These results are somewhat similar to the effect of water vapor on the material (Yan et al., 1987; Zhang et al., in preparation), which produces surface barium-rich needles (presumably barium carbonate originally) as shown in Figure 9. Both Auger and microanalysis show the surface barium, with microanalysis indicating that the perovskite frame is retained in a bulk barium-deficient

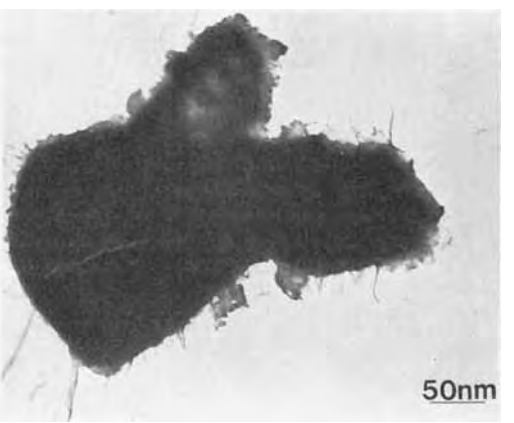

Fig. 9. A single grain of superconductor damaged by exposure to lab air for a month. Needles of barium-rich phase have grown on the surface. Similar effects can be observed on specimens exposed to very air for 30 minutes.

compound. We suspect that here again both oxygen loss and barium diffusion are important.

DISCUSSION

Perhaps the biggest problem for electron microscopists at present in the area of high Tc superconductors is that essentially all the results are negative; there is a clear negative correlation between the observed superconductivity and any crystalline defects. The current thinking in the literature is that the number and distribution of oxygen point defects is critical and oxygen unfortunately is not readily observable in the microscope. Although one can clearly in principle determine the difference between, for instance, the [100] and [010] directions in an image, determining the order/disorder characteristics of the oxygen point defects will be hard if not impossible under the microscope. Perhaps the most important role of electron microscopy is yet to come, i.e., its use in characterizing processed materials which may contain unwanted phases or characterizing metal/superconductor composites. At present, however, processing of these materials seems to be a very dark area, and we have to await further progress.

ACKNOWLEDGMENTS

This work was supported by the NSF grant number DMR 8520280.

REFERENCES

Beech, F., Miraglia, S., Santoro, A., and Roth R.S. (1987) Netron study of the crystal structure and vacancy distribution in the superconductor $Ba_2YCu_3O_{9-\delta}$. Phys. Rev. B, 35:8778–8781.

Beno, M.A., Soderholm, L., Capone D.W. II, Hinks, D.G., Jorgensen, J.D., Schuller, I.K., Segre, C.U., Zhang, K., and Grace, J.D. (1987) Structure of the single-phase high-temperature superconductor $YBa_2Cu_3O_{7-\delta}$. Appl. Phys. Lett., 51:57–59.

Beyers, R., Lim, G., Engler, E.M., Savoy, R.J., Shaw, T.M., Dinger, T.R., Gallagher, W.J., and Sandstrom, R.L. (1987) Crystallography and microstructure of $Y_1Ba_2Cu_3O_{9-x}$, a perovskite-based superconducting oxide. Appl. Phys. Lett., 50:1918–1920.

Buckett, M.I., Luzzi, D.E., Zhang, J.P., Zhang, L., and Marks, L.D. (1987) High Resolution Electron Microscopy of High Tc Superconductors at Northwestern University. Hitachi Instrument News, 12th edition, July 1987, pp. 3–8.

Eaglesham, D.J., Humphreys, C.J., Clegg, W.J., Harmer, M.A., Alford, N.McN., and Birchall, J.D. (1987) The orthorhombic and tetragonal phases of $Y_1Ba_2Cu_3O_{9-y}$. Adv. Ceram. Mater. [Suppl.], 2(3B):662–667.

Fisk, Z., Thompson, J.D., Zirngiebl, E., Smith, J.L., and Cheong, S.-W. (1987) Superconductivity of rare earth-barium-copper oxides. Solid State Commun., 62:743–744.

Gallagher, P.K., O'Bryan, H.M., Sunshine, S.A., and Murphy, D.W. (1987) Oxygen stoichiometry in $Ba_2Y_C u_3O_x$. Mater. Res. Bull., 22:995–1006.

Greedan, J.E., O'Reilly, A.H., and Stager, C.V. (1987) Oxygen ordering in the crystal structure of the 93-K superconductor $YBa_2Cu_3O_7$ using powder neutron diffraction at 298 and 79.5 K. Phys. Rev. B, 35:8770–8773.

Hazen, R.M., Finger, L.W., Angel, R.J., Prewitt, C.T., Ross, N.L., Mao, H.K., Hadidiacos, C.G., Hor, P.H., Meng, R.L., and Chu, C.W. (1987) Crystallographic description of phases in the Y-Ba-Cu-O superconductor. Phys. Rev. B, 35:7238–7241.

Hewat, E.A., Dupuy, M., Bourret, A., Capponiu, J.J., and Marezio, M. (1987) High-resolution electron microscopy of the high-temperature superconductor $YBa_2Cu_3O_7$. Nature, 327:400–402.

Hor, P.H., Meng, R.L., Wang, Y.Q., Gao, L., Huang, Z.L., Bechtold, J., Forster, K., and Chu, C.W. (1987) Superconductivity above 90K in the square-planar compound system $ABa_2Cu_3O_{6+x}$ with A=Y, La, Nd, Sm, Eu, Gd, Ho, Er, and Lu. Phys. Rev. Lett., 58:1891–1893.

Hulliger, F., and Ott, H.R. (1987) Superconducting and magnetic properties of $Ba_2LnCu_3O_{7-x}$ (Ln=Lanthanides). Z. Phys. B, 67:291–298.

Hwu, S.-J., Song, S.N., Theil, J., Poeppelmeier, K.R., Ketterson, J.B., and Freeman, A.J. (1987a) High-Tc superconductivity in regions of possible compound formation: $Y_{2-x}Ba_xCuO_{4-x/2+\delta}$ and $Y_{2-x}Ba_{1+x}Cu_2O_{6-x/2+\delta}$. Phys. Rev. B, 35:7119–7121.

Hwu, S.-J., Song, S.N., Ketterson, J.B., Mason, T.O., and Poeppelmeier, K.R. (1987b) Subsolidus compatibilities in the Y_2O_3-BaO-CuO system via diamagnetic susceptibility. J. Am. Ceram. Soc., 70:C165–167.

Hyde, B.G., Thompson, J.G., Withers, R.L., Fitzgerald, J.G., Stewart, A.M., Bevan, D.L.M., Anderson, J.S., Bitmead, J., and Paterson, M.S. (1987) The room-temperature structure of the ~90-K superconducting phase $YBa_2Cu_3O_{7-x}$. Nature, 327:402–403.

Li, D.L., and Zhang, J.P. (1987) Structure of brown polymorphs of $YBa_2Cu_3O_7$. In preparation.

Marks, L.D., Zhang, J.P., Hwu, S.-J., and Poeppelmeier, K.R. (1987) Order-disorder in $YBa_2Cu_3O_7$. J. Solid State Chem., 69:189–195.

Ourmazd, A., Rentschler, J.A., Spence, J.C.H., O'Keefe, M., Graqham, R.J., Johnson D.W., Jr., and Rhodes, W.W. (1987) Microstructure, oxygen ordering and planar defects in the high-Tc superconductor $YBa_2Cu_3O_{6.9}$. Nature, 327:308–310.

Petford, A.K., Marks, L.D., and O'Keeffe, M., (1986) Atomic imaging of oxygen desorption from tungsten trioxide. Surface Sci., 172:496–508.

Robinson, Q., Georgopoulos, P., Johnson, D.L., Marcy, H.O., Kannewurf, C.R., Hwu, S.-J., Marks, T.J., Poeppelmeier, K.R., Song, S.N., and Ketterson, J.B. (1987) Sinter-forged $YBa_2Cu_3O_{7-\delta}$. Adv. Ceram. Mater. [Suppl.], 2(3B):380–387.

Shibahara, H., Hwu, S.-J., Poeppelmeier, K.R., and Marks, L.D. (1987) Copper rich planar defects in Gd-$Ba_2Cu_3O_7$. In preparation.

Siegrist, T., Sunshine, S., Murphy, D.W., Cava, R.J., and Zahurak, S.M. (1987) Crystal structure of the high-Tc superconductor $Ba_2YCu_3O_{9-\delta}$. Phys. Rev. B, 35:7137–7139.

Wang, G., Hwu, S.-J., Song, S.N., Ketterson, J.B., Marks, L.D., Poeppelmeier, K.R., and Mason, T.O. (1987) 950 subsolidus phase diagram for Y_2O_3-BaO-CuO system in air. Adv. Ceram. Mater. [Suppl.], 2(3B):313–326.

Yan, M.F., Barns, R.L., O'Bryan, H.M., Jr., Gallagher, P.K., Sherwood, R..C, and Jin, S. (1987) Water interaction with the superconducting $YBa_2Cu_3O_7$ phase. Appl. Phys. Lett., 51:532–534.

Zandbergen, H.W., Holland, G.F., Tejedor, P., Gronsky, R., and Stacy, A.M. (1987) A Study of mixed phase behaviour in the lanthanide-substituted superconducting oxide $ErBa_2Cu_3O_7$. Adv. Ceram. Mater. [Suppl.] 2(3B):688–697.

Zhang, J.P., Li, G.P., and Marks, L.D. (1987) Electron beam and water vapour damage of $YBa_2Cu_3O_7$. In preparation.